International Journal of Mathematical Theory and Applications
Vol 1, Issue 1 2025

Algebraic methods for handling fractional coupled Equations of Navier-Stokes

Shukla[1]

1 Department of Mathematics

Article Info

Received: 31-05-2024 **Revised:08-06-2025** **Accepted:19-06-2025** **Published:30-06-2025**

Abstract: In order to get approximate analytical solutions to the Caputo-type of fractional Navier-Stokes equations, this study investigates the use of the Mohand Variational Iteration Method (MVIM) and the q-Homotopy Mohand Transform Method (q-HMTM). Two distinct sets of beginning circumstances are used to assess the adaptability of the two approaches. The q-HMTM adds an auxiliary parameter that comes to govern the convergence of the series solution, while the Mohand transformation makes it simple to handle coupled nonlinear components and deal fractional derivatives. The quantitative answers provided by both approaches are in extremely excellent agreement with the actual solutions, as shown by the tables and graphs. In solving nonlinear coupled fractional PDEs, comparative analysis demonstrates the excellent accuracy, stability, and dependability of both MVIM and q-HMTM. It also highlights the potential of the Mohand transformation as an effective analytical technique in fractional fluid dynamics.

Keywords: Fractional order differential equations, system of Navier-Stokes equations, Mohand variational

1. Introduction

Over the last several decades, researchers across a wide range of scientific and technical fields have found the power of fractional calculus (FC), which was first discovered more than three centuries ago. Its ability to include memory effects, nonlocal interactions, and hereditary features into mathematical models—all crucial for simulating large and heterogeneous systems—is the primary reason for its resurgence. Because FC extends the concept of differentiation to arbitrary (non-integer) orders, it allows mathematics to describe the dynamics of systems that classical calculus is unable to explain because of long-term temporal correlation or local spatial inhomogeneities [31, 35]. Non-integer order differential operators have been particularly helpful in simulating anomalous diffusion and transport in complex media, and their practical use in a wide range of scientific domains has been made possible by recent advances in computer power [32, 33, 52]. The domains of biomathematics have seen great success with permitted uses of FC.

[12], chaos theory [13], financial mathematics [48], optics [16], and numerous other areas of science and technology [34, 41, 42, 47, 49, 50], highlighting its practical complexity and utility.

Modeling nonlinear systems of partial differential equations (PDEs) has long been a persistent prob- lem in applied mathematics because nonlinearity together with memory effects may result in complex dynamical behavior. In this regard, fractional derivatives open up new possibilities to describe processes in the real world more accurately and flexibly. Much attention has been paid to the types of fractional derivatives, their properties, and the effect that they have on the model behavior [27, 39, 40, 46]. Pod- lubny [40] summarized some of the many diverse applications that have been realized due to fractional calculus. In epidemiology, as an example, the fractional stochastic susceptible-infective-susceptible (SIS) model of epidemic with low vaccination indicates the value of fractional modeling to reproduce realistic population dynamics. Abuasad et al. [3] also used the fractional multi-step differential transform method to approximate the solutions of this issue, and Ross [44] described the most significant conditions that define the fractional derivatives. The attempts of other researchers to

relate two or more methods in order to obtain analytical or numerical solutions have led to different suggestions of new definitions of frac- tional derivatives as well. As an illustration, variants of the beta fractional derivative have been proposed to obtain an accurate solution of time-fractional diffusion equations in several spatial dimensions [1, 2].

The fractional-order Navier-Stokes (NS) equations constitute an especially important advancement of fluid dynamics within this wider context. It is possible that by using a fractional derivative instead of the traditional time derivative (usually in the Caputo form), the fractional NS equations can bridge between classical and anomalous flows in order to model memory-dependent transport behavior more sensitively. It is the fractional extension that allows many different kinds of flow behavior to be investigated by simply varying the fractional order, and so one can model many kinds of processes between viscoelastic flows and anomalous diffusion in porous media. Notably, this flexibility also makes it possible to adjust the model to better represent data in the experiment or observation, and hence to enhance the predictive accuracy of the solutions as well as their relevance to physical experiments. The present procedures is based on the idea of applying the Mohand transformations in conjunction with the q-Homotopy analysis method and variational iteration method to fractional derivatives in the Caputo sense, so that solutions to the fractional NS system could be reconstructed in terms of different fractional orders. In such a manner, several individual distinct dynamical behaviors of the NS system can be disclosed and explored at the same time.

A number of notable contributions have been made to this field. Herrmann [23] and Hilfer [24] explained the relevance of fractional PDEs in science and engineering, and applications of fractional PDEs in other fields such as the time-fractional NS system. El-Shahed and Salem [19] were the first to model the NS equations in a fractional manner, generalizing the equations through use of Laplace, finite Hankel and finite Fourier sine transformations. Subsequently Kumar et al. [29] analytically solved a nonlinear fractional NS model by coupled with homotopy perturbation method (HPM) and Laplace transform analysis and Ganji et al. [20] and Ragab et al. [43] applied homotopy analysis method (HAM) to nonlinear time-fractional NS system. Momani and Odibat [37] and Birajdar [14] presented Adomian decomposition method (ADM) in fractional NS equations. Chaurasia and Kumar [17] have worked out solutions that employed a combination of the finite Hankel transform and Laplace transform combination, Kumar et al.
[28] have obtained analytical solutions by coupling Laplace transform with the ADM. These contributions together serve to illustrate the wide range of semi-analytical and transform based approaches that have been devised to combat the issues that fractional NS systems present.

The variational iteration method (VIM) has the advantage of being simple and general in its imple- mentation among the family of iterative analytical methods. J. H. He was the first to introduce it. It has been used with great success to many nonlinear problems of a wide nature [21, 22]. With time, VIM has been generalized to include integration with other transforms to enable dealing with fractional opera- tors more adequately resulting in the variation iteration transform method (VITM). Although VITM has been used to solve linear fractional differential equations [51] and nonlinear oscillators [11], in this paper, we augment the same by including the Mohand transform in the VIM framework to obtain a solution
method, the Mohand variational iteration method (MVIM) [45]. The use of the Mohand transform has definite advantages over other transforms normally applied in VITM [10]: it makes Caputo-type fractional derivatives easily tractable in algebraic form, evades the pernicious convolution integrals that plague con- ventional use of Laplace, Sumudu or other type of integral transforms [4, 6–9], and improves ease of formulas expressing the inversion process. This combination augments convergence, simplifies computa- tional complexity and retains nonlinear nature of the original system. In contrast with techniques such as ADM, which require calculation of the Adomian polynomials in a recursive manner [5], or the mesh point method, which limits the achievable accuracy at discrete points [18], the MVIM method exhibits convergent rates to continuous approximation of solutions with only modest overhead. Other extensions like the Shehu decomposition technique [15, 26, 30] have shown that the decomposition methods are flex- ible, though when the Mohand transform is incorporated into VIM a more effective and efficient strategy is established in finding solutions to nonlinear fractional PDEs as we shall see in the fractional-order Navier-Stokes system treated here.

The analytical power of the q-homotopy Mohand transform method (q-HMTM) in solving fractional PDEs is also outlined in this work. The q-HMTM takes the versatility of the homotopy analysis method and the efficiency of the Mohand transform (MT). Its greatest strength is its capability to quickly build up series of convergent solutions through combining two complementary strategies. Whereas classical integral transforms (like those of Fourier and Laplace) are well studied, MT is a more recent transform whose operations rules are distinct. It is distinguished among other transforms by its property of unity which eases algebraic manipulations of fractional derivatives. In contrast to Laplace and Sumudu trans- forms which sometimes lead to complicated inverse formulas with Mittag-Leffler functions, the Mohand transform tends to conserve compact recursive form and simpler inversion. Consequently, fractional non- linear PDEs using MT-based hybrid methods typically have lower computational cost and smaller CPU time. The MT-based combination of the semi-analytical methods VIM, q-homotopy allows simplifying the fractional operators together with fast convergence.

In this paper, q-HMTM and MVIM are applied to the fractional-order NS equations within the frame- work of the Caputo fractional order derivative. The innovation with regard to this work is use of the Mohand transform as the primary operator that possesses desirable properties compared to the conven- tional transforms. The numerical experiments typical of the proposed methods performance are provided in details including tables and graphical illustrations that tend to verify the

convergence and accuracy of the solution. The comparison between integer-order and fractional-order cases indicate the effects of the fractional parameter and demonstrate the smooth combination of transitions across the regimes of the pro- posed hybrid methods. Finally, the methods established in this context offer a powerful semi-analytical treatment not just in the context of fractional NS equations but even more general classes of nonlinear fractional PDEs.

1. Concepts of Mohand transform

$$M[u(t)] = R(s) = s^2 \int_0^{\infty} u(t) e^{-st}\, dt, \quad k_1 \leqslant s \leqslant k_2.$$

A brief expression of the inverse MT (MIT) is as $M^{-1}[R(s)] = u(t)$.

Definition 2.2 ([38])**.** The MT fractional order derivative is expressed as:

$$M[u^{\psi}(t)] = s^{\psi}R(s) - \sum_{k=0}^{n-1} \frac{u^{k}(0)}{s^{k-(\psi+1)}}, \quad 0 < \psi \leqslant n.$$

Definition 2.3. A few of the characteristics of the MT are given below:

1. $M[u'(t)] = sR(s) - s^2R(0)$;
2. $M[u''(t)] = s^2R(s) - s^3R(0) - s^2R'(0)$;
3. $M[u^n(t)] = s^nR(s) - s^{n+1}R(0) - s^nR'(0) - \cdots - s^nR^{n-1}(0)$.

Lemma 2.4. *Let* $u(y, t)$ *be an exponentially ordered function. The MT is thus defined as ([25])*

$$M[D_t^{r\psi}u(y, t)] = s^{r\psi}R(s) - \sum_{j=0}^{r-1} s^{\psi(r-j)-1}D^{j\psi}u_t(y, 0), \quad 0 < \psi \leqslant 1, \tag{2.1}$$

where $y = (y_1, y_2, \ldots, y_{\psi}) \in R^{\psi}$ *and* $\psi \in N$ *and* $D^{r\psi} = D^{\psi}.D^{\psi}.\cdots.D^{\psi}$ *(r-times).*

Lemma 2.5. *Let us assume that* $u(y, t)$ *has an exponential order.* $M[u(y, t)] = R(s)$ *denotes the MT of* $u(y, t)$*. In relation to the Mohand transform, the multiple fractional power series (MFPS) is written as follows:*

$$R(s) = \sum_{r=0}^{\infty} \frac{\hbar_r(y)}{s^{r\psi+1}}, \quad s > 0,$$

where $y = (s_1, y_2, \ldots, y_{\psi}) \in R^{\psi}$, $\psi \in N$.

Proof. Consider the Taylor series:

$$u(y, t) = \tilde{h}_0(y) + \tilde{h}_1(y) \frac{t^{\psi}}{\Gamma[\psi+1]} + \tilde{h}_2(y) \frac{t^{2\psi}}{\Gamma[2\psi+1]} + \cdots. \tag{2.2}$$

By employing MT on equation (2.2), we obtain the subsequent outcome:

$$M[u(y, t)] = M[\hbar_0(y)] + M\left[\hbar_1(y) \frac{t^{\psi}}{\Gamma[\psi+1]}\right] + M\left[\hbar_1(y) \frac{t^{2\psi}}{\Gamma[2\psi+1]}\right] + \cdots.$$

The MT features lead to the following result:

$$M[u(y, t)] = \tilde{h}_0(y) \frac{1}{s} + \tilde{h}_1(y) \frac{\Gamma[\psi+1]}{\Gamma[\psi+1]} \frac{1}{s^{\psi+1}} + \tilde{h}_2(y) \frac{\Gamma[2\psi+1]}{\Gamma[2\psi+1]} \frac{1}{s^{2\psi+1}} \cdots.$$

Thus, we get a new Taylor series. □

Lemma 2.6. *Assuming that MT is represented by* $M[u(y, t)] = R(s)$*, the new Taylor series in MFPS is as follows:*

$$\hbar_0(y) = \lim_{s \to \infty} sR(s) = u(y, 0). \tag{2.3}$$

Proof. Assume the Taylor series:

$$\hbar_0(y) = sR(s) - \frac{\hbar_1(y)}{s^{\psi}} - \frac{\hbar_2(y)}{s^{2\psi}} - \cdots . \tag{2.4}$$

Equation (2.4) is the result of computing and simplifying the limit found in equation (2.3). □

Theorem 2.7. *Consider* $M[u(y,t)]$ *represents a function. Then,* $R(s)$ *is denoted in MFPS form as follows:*

$$R(s) = \sum_{r=0}^{\infty} \frac{\hbar_r(y)}{s^{r\psi+1}}, \quad s > 0,$$

where $y = (y_1, y_2, \ldots, y_{\psi}) \in R^{\psi}$ *and* $\psi \in N$. *Then we have* $\hbar_r(y) = D^{r\psi}u(y,0)$, *where* $D^{r\psi} = D^{\psi}.D^{\psi}.\cdots.D^{\psi}$

(r-times). D_t^{ψ} $D_t^{2\psi}$ $D_t^{r\psi}$

Proof. Assume the Taylor series:

$$\hbar_1(y) = s^{\psi+1}R(s) - s^{\psi}\hbar_0(y) - \frac{\hbar_2(y)}{s^{\psi}} - \frac{\hbar_3(y)}{s^{2\psi}} - \cdots. \tag{2.5}$$

The subsequent result is obtained by applying the limit to equation (2.5):

$$\hbar_1(y) = \lim_{s\to\infty}(s^{\psi+1}R(s) - s^{\psi}\hbar_0(y)) - \lim_{s\to\infty}\frac{\hbar_2(y)}{s^{\psi}} - \lim_{s\to\infty}\frac{\hbar_3(y)}{s^{2\psi}} - \cdots.$$

After simplification, we obtain:

$$\hbar_1(y) = \lim_{s\to\infty}(s^{\psi+1}R(s) - s^{\psi}\hbar_0(y)). \tag{2.6}$$

The following version of equation (2.6) can be formed by employing the fundamental concepts delineated in Lemma 2.4:

$$\hbar_1(y) = \lim_{s\to\infty}(sM[D^{\psi}u(y,t)](s)). \tag{2.7}$$

The foundation for equation (2.7) is Lemma 2.5:

$$\hbar_1(y) = D^{\psi}u(y,0).$$

Again, the Taylor series must be applied and $\lim_{s\to\infty}$ is taken in order to obtain the subsequent outcome,

$$\hbar_2(y) = s^{2\psi+1}R(s) - s^{2\psi}\hbar_0(y) - s^{\psi}\hbar_1(y) - \frac{\hbar_3(y)}{s^{\psi}} - \cdots.$$

Lemma 2.5 is employed to acquire the subsequent outcomes:

$$\hbar_2(y) = \lim_{s\to\infty}(s^{2\psi}R(s) - s^{2\psi-1}\hbar_0(y) - s^{\psi-1}\hbar_1(y)). \tag{2.8}$$

The equation (2.8) is modified in the following manner, based on Lemmas 2.4 and 2.6:

$$\hbar_2(y) = D^{2\psi}u(y,0).$$

The same procedure is followed to obtain the following: $\hbar_3(y) = \lim_{s\to\infty} s(M[D^{2\psi}u(y,\psi)](s))$. The final solution is obtained by employing Lemma 2.6 as $D_t^{r\psi}u(y,0)$. Generally $\hbar_3(y) = D_t^{3\psi}u(y,0)$ $\hbar_r(y) = D_t^{r\psi}u(y,0)$ So the theorem is proved. □

The following theorem elucidates and describes the novel form of Taylor's series convergence.

Theorem 2.8. *The MFTS expression is characterized by the application of Lemma* 2.5*, as illustrated:* $M[u(t,y)] = R(s)$. *When* $|s^a M[D_t^{(K+1)\psi}u(y,t)]| \leqslant T$, *for all* $s > 0$ *and* $0 < \psi \leqslant 1$, *the residual* $H_K(y,s)$ *of the MFTS satisfies the inequality:*

$$|H_K(y,s)| \leqslant \frac{T}{s^{(K+1)\psi+1}}, \quad s > 0.$$

Proof. Let $M[D_t^{r\psi}u(y,t)](s)$ is defined on $s>0$ for $r=0,1,2,\ldots,K+1$ and consider $|sM[D_{t^{K+1}}u(y,t)]| \leqslant T$. The new Taylor series may be employed to identify the resulting relationship.

$$H_K(y,s) = R(s) - \sum_{r=0}^{K} \frac{h_r(y)}{s^{r\psi+1}}. \tag{2.9}$$

Equation (2.9) and the Theorem 2.7 can be used to obtain the following outcome:

$$H_K(y,s) = R(s) - \sum_{r=0}^{K} \frac{D_t^{r\psi}u(y,0)}{s^{r\psi+1}}. \tag{2.10}$$

In the following step, we multiply $s^{(K+1)a+1}$ with equation (2.10):

$$s^{(K+1)\psi+1}H_K(y,s) = s(s^{(K+1)\psi}R(s) - \sum_{r=0}^{K} s^{(K+1-r)\psi-1}D_t^{r\psi}u(y,0)), \tag{2.11}$$

A new form of equation (2.11) is obtained by using Lemma 2.4:

$$s^{(K+1)\psi+1}H_K(y,s) = sM[D_t^{(K+1)\psi}u(y,t)].$$

Take the absolute:

$$|s^{(K+1)\psi+1}H_K(y,s)| = |sM[D_t^{(K+1)\psi}u(y,t)]|. \tag{2.12}$$

In order to achieve the desired outcome, the condition of equation (2.12) must be implemented,

$$\frac{-T}{s^{(K+1)\psi+1}} \leqslant H_K(y,s) \leqslant \frac{T}{s^{(K+1)\psi+1}}. \tag{2.13}$$

Another way to express the outcome of equation (2.13) is as $|H_K(y,s)| \leqslant \frac{T}{s^{(K+1)\psi+1}}$. Consequently, a distinctive condition for the series' convergence is established. □

2. Methodology

2.1. *General methodology of* q-*HMTM*

Let suppose the nonhomogeneous, nonlinear system of PDEs of the fractional order:

$$\begin{aligned} &D_t^{\psi}u_1(y,t) + R_1u_1(y,t) + N_1u_1(y,t) = g_1(y,t),\\ &D_t^{\psi}u_2(y,t) + R_2u_2(y,t) + N_2u_2(y,t) = g_2(y,t), \quad n-1 < \psi \leqslant n. \end{aligned} \tag{3.1}$$

Here, $D_t^{\psi}u_1(y,t)$ and $D_t^{\psi}u_2(y,t)$ denote the derivative of Caputo, whereas N_1 and N_2 are nonlinear operators and R_1 and R_2 denote the linear operators, and the source terms are $g_1(y,t)$ and $g_2(y,t)$. Subject the Mohand transformation to equation (3.1),

$$M[u_1(y,t)] - \frac{1}{s^{\psi}}\sum_{k=0}^{n-1} s^{\psi-k-1}u_1^k(y,0) + \frac{1}{s^{\psi}}[M[R_1u_1(y,t)] + M[N_1u_1(y,t)] - M[g_1(y,t)]] = 0,$$

$$M[u_2(y,t)] - \frac{1}{s^{\psi}}\sum_{k=0}^{n-1} s^{\psi-k-1}u_2^k(y,0) + \frac{1}{s^{\psi}}[M[R_2u_2(y,t)] + M[N_2u_2(y,t)] - M[g_2(y,t)]] = 0.$$

The following are the description of the non-linear operators:

$$N[\varphi_1(y,t;q)] = M[\varphi_1(y,t;q)] - \frac{1}{s^{\psi}}\sum_{k=0}^{n-1} s^{\psi-k-1}\varphi_1^{k}(y,t;q)(0^+) + \frac{1}{s^{\psi}}[M[R_1\varphi_1(y,t;q)] + M[N_1\varphi_1(y,t;q)] - M[g_1(y,t)]],$$

$$N[\varphi_2(y,t;q)] = M[\varphi_2(y,t;q)] - \frac{1}{s^{\psi}}\sum_{k=0}^{n-1} s^{\psi-k-1}\varphi_2^{k}(y,t;q)(0^+) + \frac{1}{s^{\psi}}[M[R_2\varphi_2(y,t;q)] + M[N_2\varphi(y,t;q)] - M[g_2(y,t)]].$$

Where the real valued function with respect to y, t, and $q \in [0, \frac{1}{n}]$ are $\varphi_1(y,t;q))$ and $\varphi_2(y,t;q))$ and defining the homotopy as:

$$(1-nq)M[\varphi_1(y,t;q) - u_{10}(y,t)] = \hbar q\, h_1(y,t)N_1[\varphi_1(y,t;q)],$$

$$-nq)M[\varphi_2(y,t;q)-u_{20}(y,t)]=\hbar\, q\ h_2(y,t)N_2[\varphi_2(y,t;q)]. \tag{3.2}$$

The auxiliary parameter in the preceding equation is $\hbar$ $= 0$, and the starting conditions are u_{10} and u_{20}.

The following outcomes are true for both $\frac{1}{n}$ and 0:

$$\varphi_1(y,t;0)=u_{10}(y,t),\quad \varphi_1(y,t;\tfrac{1}{n})=u_1(y,t),\qquad \varphi_2(y,t;0)=u_{20}(y,t),\quad \varphi_2(y,t;\tfrac{1}{n})=u_2(y,t).$$

Due to the intensification of q, the solutions $\varphi_1(y,t;q)$ and $\varphi_2(y,t;q)$ are different from the first estimate $u_{10}(y,t)$ to $u_1(y,t)$ and $u_{20}(y,t)$ to $u_2(y,t)$. The following may be obtained by implementing the Taylor theorem to $\varphi_1(y,t;q)$ and $\varphi_2(y,t;q)$ in relation to q:

$$\varphi_1(y,t;q)=u_{10}(y,t)+\sum_{m=1}^{\infty}u_{1m}(y,t)q^m,\qquad \varphi_2(y,t;q)=u_{20}(y,t)+\sum_{m=1}^{\infty}u_{2m}(y,t)q^m,$$

where

$$u_{1m}=\frac{1}{m!}\frac{\partial^m\varphi_1(y,t;q)}{\partial q^m}\Big|_{q=0}\quad\text{and}\quad u_{2m}=\frac{1}{m!}\frac{\partial^m\varphi_2(y,t;q)}{\partial q^m}\Big|_{q=0}.$$

For suitable values of $u_{10}(y,t)$, $u_{20}(y,t)$, n, and $\hbar$, the series (3.2) converges at $q=\frac{1}{n}$ and

$$\varphi_1(y,t;q)=u_{10}(y,t)+\sum_{m=1}^{\infty}u_{1m}(y,t)\left(\frac{1}{n}\right)^m,\qquad \varphi_2(y,t;q)=u_{20}(y,t)+\sum_{m=1}^{\infty}u_{2m}(y,t)\left(\frac{1}{n}\right)^m.$$

We calculate the derivative of equation (3.2) with respect to the embedding parameter q by setting $q=0$, and dividing by m!:

$$\begin{aligned}M[u_{1m}(y,t)-k_m u_{1m-1}(y,t)]&=\hbar h_1(y,t)R_{1m}(\vec{u}_{1m-1}),\\ M[u_{2m}(y,t)-k_m u_{2m-1}(y,t)]&=\hbar h_2(y,t)R_{2m}(\vec{u}_{2m-1}),\end{aligned}\tag{3.3}$$

Auxiliary parameter $\hbar\neq 0$ and the vectors are defined as follows:

$$\vec{u}_{1m}=[u_1(y,t),u_{11}(y,t),\ldots,u_{1m}(y,t)],\qquad \vec{u}_{2m}=[u_{20}(y,t),u_{21}(y,t),\ldots,u_{2m}(y,t)].$$

When equation (3.3) is subjected to the inverse Mohand transform, the following is the result:

$$\begin{aligned}u_{1m}(y,t)&=k_m u_{1m-1}(y,t)+\hbar M^{-1}[h_1(y,t)R_{1m}(\vec{u}_{1m-1})],\\ u_{2m}(y,t)&=k_m u_{2m-1}(y,t)+\hbar M^{-1}[h_2(y,t)R_{2m}(\vec{u}_{2m-1})],\\ \vec{R}_{1m}(u_{1m-1})&=\frac{1}{(m-1)!}\frac{\partial^{m-1}N_1[\varphi_1(y,t;q)]}{\partial q^{m-1}}\Big|_{q=0},\\ \vec{R}_{2m}(u_{2m-1})&=\frac{1}{(m-1)!}\frac{\partial^{m-1}N_2[\varphi_2(y,t;q)]}{\partial q^{m-1}}\Big|_{q=0},\\ k_m&=\begin{cases}0, & \text{if } m\leqslant 1,\\ 1, & \text{if } m>1.\end{cases}\end{aligned}\tag{3.4}$$

Equation (3.4) must be solved in order to ascertain the components of the q-HMTM solution.

2.2. *General methodology of MVIM*

Let suppose the nonhomogeneous, nonlinear system of PDEs of the fractional order:

$$\begin{aligned}D_t^{\psi}u_1(y,t)&=R_1u_1(y,t)+N_1u_1(y,t)+g_1(y,t),\\ D_t^{\psi}u_2(y,t)&=R_2u_2(y,t)+N_2u_2(y,t)+g_2(y,t),\quad n-1<\psi\leqslant n.\end{aligned}\tag{3.5}$$

Initial conditions are $u_1(y,0) = u_{1n-1}(y)$, $u_2(y,0) = u_{2n-1}(y)$. By using the Mohand transform on equation (3.5), the subsequent outcome is achieved:

$$M[D^{\psi}u_1(y,t)] = M[R_1u_1(y,t) + Nu_1(y,t) + g_1(y,t)],$$
$$M[D^{\psi}u_2(y,t)] = M[R_2u_2(y,t) + Nu_2(y,t) + g_2(y,t)].$$

Using the transform's iteration property, we achieve the following outcome:

$$\begin{aligned} M[u_1(y,t)] - \sum_{k=0}^{m-1} s^{\psi-k-1} \frac{\partial^k u_1(y,t)}{\partial t^k}\Big|_{t=0} &= M[R_1u_1(y,t) + N_1u_1(y,t) + g_1(y,t)], \\ M[u_2(y,t)] - \sum_{k=0}^{m-1} s^{\psi-k-1} \frac{\partial^k u_2(y,t)}{\partial t^k}\Big|_{t=0} &= M[R_2u_2(y,t) + N_2u_2(y,t) + g_2(y,t)]. \end{aligned} \tag{3.6}$$

The Lagrange multiplier $(-\lambda(s))$ is integrated iteratively to obtain:

$$\begin{aligned} M[u_{1n+1}(y,t)] &= M[u_{1n}(y,t)] - \lambda(s)\left[M[u_{1n}(y,t)] - \sum_{k=0}^{m-1} s^{\psi-k-1} \frac{\partial^k u_1(y,0)}{\partial t^k}\right], \\ M[u_{2n+1}(y,t)] &= M[u_{2n}(y,t)] - \lambda(s)\left[M[u_{2n}(y,t)] - \sum_{k=0}^{m-1} s^{\psi-k-1} \frac{\partial^k u_2(y,0)}{\partial t^k}\right]. \end{aligned} \tag{3.7}$$

Equation (3.7) is substituted into equation (3.6) provided that $\lambda(s) = -\frac{1}{s^{\psi}}$,

$$\begin{aligned} M[u_{1n+1}(y,t)] &= M[u_{1n}(y,t)] - \lambda(s)\left[M[u_{1n}(y,t)]\right. \\ &\quad \left. - \sum_{k=0}^{m-1} s^{\psi-k-1} \frac{\partial^k u_1(y,0)}{\partial t^k} + M[R_1u_1(y,t) + N_1u_1(y,t) + g_1(y,t)]\right], \\ M[u_{2n+1}(y,t)] &= M[u_{2n}(y,t)] - \lambda(s)\left[M[u_{2n}(y,t)]\right. \\ &\quad \left. - \sum_{k=0}^{m-1} s^{\psi-k-1} \frac{\partial^k u_2(y,0)}{\partial t^k} + M[R_2u_2(y,t) + N_2u_2(y,t) + g_2(y,t)]\right], \end{aligned} \tag{3.8}$$

We may obtain the following by applying the Mohand inverse transform on equation (3.8):

$$\begin{aligned} u_{1n+1}(y,t) &= u_{1n}(y,t) + M^{-1}\left[\frac{1}{s^{\psi}}\left(\sum_{k=0}^{m-1} s^{\psi-k-1} \frac{\partial^k u_1(y,0)}{\partial t^k} + M[R_1u_1(y,t) + N_1u_1(y,t) + g_1(y,t)]\right)\right], \\ u_{2n+1}(y,t) &= u_{2n}(y,t) + M^{-1}\left[\frac{1}{s^{\psi}}\left(\sum_{k=0}^{m-1} s^{\psi-k-1} \frac{\partial^k u_2(y,0)}{\partial t^k} + M[R_2u_2(y,t) + N_2u_2(y,t) + g_2(y,t)]\right)\right]. \end{aligned}$$

We get the initial conditions as:

$$u_{10}(y,t) = M^{-1}\left[\frac{1}{s^{\psi}}\sum_{k=0}^{m-1} s^{\psi-k-1} \frac{\partial^k u_1(y,0)}{\partial t^k}\right], \quad u_{20}(y,t) = M^{-1}\left[\frac{1}{s^{\psi}}\sum_{k=0}^{m-1} s^{\psi-k-1} \frac{\partial^k u_2(y,0)}{\partial t^k}\right].$$

The iterative scheme is given as:

$$\begin{aligned} u_{1n+1}(y,t) &= u_{1n}(y,t) + M^{-1}\left[\frac{1}{s^{\psi}}\left(\sum_{k=0}^{m-1} s^{\psi-k-1} \frac{\partial^k u_1(y,0)}{\partial t^k} + M[R_1u_1(y,t) + N_1u_1(y,t) + g_1(y,t)]\right)\right], \\ u_{2n+1}(y,t) &= u_{2n}(y,t) + M^{-1}\left[\frac{1}{s^{\psi}}\left(\sum_{k=0}^{m-1} s^{\psi-k-1} \frac{\partial^k u_2(y,0)}{\partial t^k} + M[R_2u_2(y,t) + N_2u_2(y,t) + g_2(y,t)]\right)\right]. \end{aligned} \tag{3.9}$$

3. Numerical example 1

3.1. *Utilization of* q-*HMTM*

Assume the NS equation of time fractional order:

$$\begin{aligned} &D_t u_1 - a\frac{\partial^2 u_1}{\partial y^2} - a\frac{\partial^2 u_1}{\partial z^2} + u_2\frac{\partial u_1}{\partial z} + u_1^{\psi}\frac{\partial u_1}{\partial y} - q = 0, \\ &D_t^{\psi} u_2 - a\frac{\partial^2 u_2}{\partial y^2} - a\frac{\partial^2 u_2}{\partial z^2} + u_1\frac{\partial u_2}{\partial y} + u_2\frac{\partial u_2}{\partial z} + q = 0, \end{aligned} \tag{4.1}$$

where $0 < \psi \leqslant 1$. IC's are given as:

$$\begin{aligned} u_1(y, z, 0) &= -e^{y+z}, \\ u_2(y, z, 0) &= e^{y+z}, \end{aligned}$$

$$M[u_1] - s\,e^{y+z} + \frac{1}{s^{\psi}}M^{h}\left[-a\frac{\partial^2 u_1}{\partial y^2} - a\frac{\partial^2 u_1}{\partial z^2} + u_2\frac{\partial u_1}{\partial z} + u_1\frac{\partial u_1}{\partial y} - q\right]^{i} = 0,$$

$$M[u_2] + s\,e^{y+z} + \frac{1}{s^{\psi}}M^{h}\left[-a\frac{\partial^2 u_2}{\partial y^2} - a\frac{\partial^2 u_2}{\partial z^2} + u_1\frac{\partial u_2}{\partial y} + u_2\frac{\partial u_2}{\partial z} + q\right]^{i} = 0.$$

The non-linear operator is defined as:

$$\begin{aligned} &N^1[\varphi_1(y, z, t; q), \varphi_2(y, z, t; q)] \\ &= M[\phi_1(y, z, t; q)] - s\,e^{y+z} + \frac{1}{s^{\psi}}M^{h}\left[-a\frac{\partial^2\varphi_1(y, z, t; q)}{\partial y^2} - a\frac{\partial^2\varphi_1(y, z, t; q)}{\partial z^2} + \varphi_2(y, z, t; q)\frac{\partial\varphi_1(y, z, t; q)}{\partial z} + \varphi_1(y, z, t; q)\frac{\partial\varphi_1(y, z, t; q)}{\partial y} - q\right]^{i}, \\ &N^2[\varphi_1(y, z, t; q), \varphi_2(y, z, t; q)] \\ &= M[\phi_2(y, z, t; q)] + s\,e^{y+z} + \frac{1}{s^{\psi}}M^{h}\left[-a\frac{\partial^2\varphi_2(y, z, t; q)}{\partial y^2} - a\frac{\partial^2\varphi_2(y, z, t; q)}{\partial z^2} + \varphi_1(y, z, t; q)\frac{\partial\varphi_2(y, z, t; q)}{\partial y} + \varphi_2(y, z, t; q)\frac{\partial\varphi_2(y, z, t; q)}{\partial z} + q\right]^{i}. \end{aligned}$$

The Mohand operator is define as:

$$\begin{aligned} M[u_1]_m - k_m u_{1\,m-1} &= \hbar\, h(y, z, t) R_{1,m}[\vec{u}_{1\,m-1}, \vec{u}_{2\,m-1}], \\ M[u_2]_m - k_m u_{2\,m-1} &= \hbar\, h(y, z, t) R_{2,m}[u'_{1\,m-1}, u'_{2\,m-1}]. \end{aligned}$$

Here,

$$\begin{aligned} \vec{R}_{1,m}[u_{1m-1}, u_{2m-1}] &= M[u_{1m-1}] - s\left(1 - \frac{k_m}{n}\right)e^{y+z} + \frac{1}{s^{\psi}}M^{h}\left[-a\frac{\partial^2 u_{1m-1}}{\partial y^2} - a\frac{\partial^2 u_{1m-1}}{\partial z^2} + \sum_{i=0}^{m-1} u_{2i}\frac{\partial u_{1m-1-i}}{\partial z} + \sum_{i=0}^{m-1} u_{1i}\frac{\partial u_{1m-1-i}}{\partial y} - q\right]^{i}, \\ \vec{R}_{2,m}[u_{1m-1}, u_{2m-1}] &= M[u_{2m-1}] + s\left(1 - \frac{k_m}{n}\right)e^{y+z} + \frac{1}{s^{\psi}}M^{h}\left[-a\frac{\partial^2 u_{2m-1}}{\partial y^2} - a\frac{\partial^2 u_{2m-1}}{\partial z^2} + \sum_{i=0}^{m-1} u_{1i}\frac{\partial u_{2m-1-i}}{\partial y} + \sum_{i=0}^{m-1} u_{2i}\frac{\partial u_{2m-1-i}}{\partial z} + q\right]^{i}, \end{aligned}$$

$$u_{1m} = k_m u_{1m-1} + \hbar M^{-1}[h(y,z,t)R_{1,m}(\vec{u}_{m-1}, \vec{u}_{1m-1}), \quad 2 \qquad (4.2)$$

$$u_2 \quad = k_m u_2 \quad {}_1 + \hbar M^{-1}[h(y,z,t)R_{2,m}(\vec{u}_{mm+}, \vec{u}_{m-1}). \quad 1 \quad 2$$

With the help of initial condition (4.2) we obtain the subsequent outcome:

$$u_{11} = \frac{\hbar t^{\psi}(2ae^{y+z} - q)}{\Gamma(\psi+1)}, \qquad u_{21} = \frac{\hbar t^{\alpha}\ q - 2ae^{y+\psi}}{\Gamma(\psi+1)},$$

$$u_{12} = \hbar t^{\psi}\frac{(n+\hbar)(2ae^{y+z} - q)}{\Gamma(\psi+1)} - \frac{4a^{2}\hbar t^{\psi}e^{y+z}}{\Gamma(2\psi+1)}, \quad u_{22} = \hbar t^{\psi}\frac{4a^{2}\hbar t^{\psi}e^{y+z}}{\Gamma(2\psi+1)} + \frac{(n+\hbar)(q - 2ae^{y+z})}{\Gamma(\psi+1)},$$

and so on. The solution of equation (4.1), as determined by q-HMTM, is as follows:

$$u_1 = u_{10} + \sum_{m=1}^{\infty} u_{1m}\left(\frac{1}{n}\right)^m, \quad u_2 = u_{20} + \sum_{m=1}^{\infty} u_{2m}\left(\frac{1}{n}\right)^m.$$

For $\psi = 1$, $\hbar = -1$, and $n = 1$ solutions $\sum_{m=1}^{N} u_1 m \left(\frac{1}{n}\right)^m$ and $\sum_{m=1}^{N} u_2 m \left(\frac{1}{n}\right)^m$ converge to the exact solutions as $N \to$,

$$u_1(y,z,t) = -e^{y+z} + \frac{\hbar t^{\psi}(2ae^{y+z} - q)}{\Gamma(\psi+1)} + \hbar t^{\psi}\frac{(n+\hbar)(2ae^{y+z} - q)}{\Gamma(\psi+1)} - \frac{4a^{2}\hbar t^{\psi}e^{y+z}}{\Gamma(2\psi+1)} + \cdots = -e^{2at+y+z},$$

$$u_2(y,z,t) = e^{y+z} + \frac{\hbar t^{\alpha}\ q - 2ae^{y+\psi}}{\Gamma(\psi+1)} + \hbar t^{\psi}\frac{4a^{2}\hbar t^{\psi}e^{y+z}}{\Gamma(2\psi+1)} + \frac{(n+\hbar)(q - 2ae^{y+z})}{\Gamma(\psi+1)} + \cdots = e^{2at+y+z}.$$

3.2. *Utilization of MVIM*

Assume the NS equation of time fractional order:

$$D_t^{\psi} u_1 = a\frac{\partial^2 u_1}{\partial y^2} + a\frac{\partial^2 u_1}{\partial z^2} - u_2\frac{\partial u_1}{\partial z} - u_1\frac{\partial u_1}{\partial y} - q, \qquad D_t^{\psi} u_2 = a\frac{\partial^2 u_2}{\partial y^2} + a\frac{\partial^2 u_2}{\partial z^2} - u_1\frac{\partial u_2}{\partial y} - u_2\frac{\partial u_2}{\partial z} + q,$$

where $0 < \psi \leqslant 1$. IC's are given as: $u_1(y, z, 0) = -e^{y+z}$, $u_2(y, z, 0) = e^{y+z}$. Using the iterative formula found in equation (3.9), we can obtain

$$u_{1n+1} = u_{1n} + M^{-1}\left[\frac{1}{s^{\psi}}\right]\left[\sum_{k=0}^{n-1} s^{\psi-k-1}\frac{\partial^k u_1(y,z,0)}{\partial t^k} + M\left[a\frac{\partial^2 u_{1n}}{\partial y^2} + a\frac{\partial^2 u_{1n}}{\partial z^2} - u_{2n}\frac{\partial u_{1n}}{\partial z} - u_1\frac{\partial u_{1n}}{\partial y} - q\right]\right],$$

$$u_{2n+1} = u_{2n} + M^{-1}\left[\frac{1}{s^{\psi}}\right]\left[\sum_{k=0}^{n-1} s^{\psi-k-1}\frac{\partial^k u_2(y,z,0)}{\partial t^k} + M\left[a\frac{\partial^2 u_{2n}}{\partial y^2} + a\frac{\partial^2 u_{2n}}{\partial z^2} - u_{1n}\frac{\partial u_{2n}}{\partial y} - u_2\frac{\partial u_{2n}}{\partial z} + q\right]\right].$$

Inserting $n = 0$ into the expression above results in the second approximation:

$$u_{11} = u_{10} + M^{-1}\left[\frac{1}{s^{\psi}}\right]\left[\sum_{k=0}^{n-1} s^{\psi-k-1}\frac{\partial^k u_1(y,z,0)}{\partial t^k} + M\left[a\frac{\partial^2 u_{10}}{\partial y^2} + a\frac{\partial^2 u_{10}}{\partial z^2} - u_{20}\frac{\partial u_{10}}{\partial z} - u_{10}\frac{\partial u_{10}}{\partial y} - q\right]\right],$$

$$= u_{20} + M^{-1}\left[\frac{1}{s^{\psi}}\right]\left[\sum_{k=0}^{n-1} s^{\psi-k-1}\frac{\partial^k u_2(y,z,0)}{\partial t^k} + M\left[a\frac{\partial^2 u_{20}}{\partial y^2} + a\frac{\partial^2 u_{20}}{\partial z^2} - u_{10}\frac{\partial u_{20}}{\partial y} - u_{20}\frac{\partial u_{20}}{\partial z} + q\right]\right].$$

By simplification, we get

$$u_{11} = \frac{-2at^{\psi}e^{y+z} + qt^{\psi} - \Gamma(\psi+1)e^{y+z}}{\Gamma(\psi+1)}, \quad u_{21} = \frac{2at^{\psi}e^{y+z} - qt^{\psi} + \Gamma(\psi+1)e^{y+z}}{\Gamma(\psi+1)}$$

By inserting n = 1, we have

$$u_{12} = u_{11} + \mathcal{M}\left[u_{22-1}^{h}\frac{1}{s^{\psi}}\sum_{k=0}^{n-1} s^{\psi-k-1}\frac{\partial^k u_1(y,z,0)}{\partial t^k} + \mathcal{M}\left[a\frac{\partial^2 u_{11}}{\partial y^2} + a\frac{\partial^2 u_{11}}{\partial z^2} - u_{21}\frac{\partial u_{11}}{\partial z} - u_{11}\frac{\partial u_{11}}{\partial y} - q\right], i\right.$$

$$\left. = u_{21} + \mathcal{M}\left[{}_{-1}^{h}\frac{1}{s^{\psi}}\sum_{k=0}^{n-1} s^{\psi-k-1}\frac{\partial^k u_2(y,z,0)}{\partial t^k} + \mathcal{M}\left[a\frac{\partial^2 u_{21}}{\partial y^2} + a\frac{\partial^2 u_{21}}{\partial z^2} - u_{11}\frac{\partial u_{21}}{\partial y} - u_{21}\frac{\partial u_{21}}{\partial z} + q\right], i\right.\right.$$

By simplifying the expression, we achieve the subsequent final outcome:

$$u_{12}(y,z,t) = -e^{y+z}\left(-\frac{2at^{\psi}e^{y+z}}{\Gamma(\psi+1)} + \frac{qt^{\psi}}{\Gamma(\psi+1)} - \frac{4a^2t^{2\psi}e^{y+z}}{\Gamma(2\psi+1)}\right)$$

$$u_{22}(y,z,t) = e^{y+z}\left(+\frac{2at^{\psi}e^{y+z}}{\Gamma(\psi+1)} - \frac{qt^{\psi}}{\Gamma(\psi+1)} + \frac{4a^2t^{2\psi}e^{y+z}}{\Gamma(2\psi+1)}\right)$$

Table 1: q-HMTM and MVIM solution error comparison of $u_1(y,z,t)$ at $z = 0.1$ and $\hbar = -1$.

t	y	MVIM$_{\psi=0.6}$	q-HMTM$_{\psi=0.6}$	MVIM$_{\psi=1}$	q-HMTM$_{\psi=1}$	Exact	MVIM Error$_{\psi=1}$	q-HMTM Error$_{\psi=1}$
	-1.0	-0.408865	-0.408865	-0.407384	-0.407384	-0.407384	5.423639×10^{-10}	5.423640×10^{-10}
	-0.5	-0.674104	-0.674104	-0.671662	-0.671662	-0.671662	8.942070×10^{-10}	8.942071×10^{-10}
0.1	0.0	-1.111410	-1.111410	-1.107380	-1.107380	-1.107380	1.474298×10^{-9}	1.474298×10^{-9}
	0.5	-1.832410	-1.832410	-1.825770	-1.825770	-1.825770	2.430706×10^{-9}	2.430706×10^{-9}
	1.0	-3.021130	-3.021130	-3.010180	-3.010180	-3.010180	4.007557×10^{-9}	4.007558×10^{-9}
	-1.0	-0.412638	-0.412638	-0.410656	-0.410656	-0.410656	6.793135×10^{-8}	6.793135×10^{-8}
	-0.5	-0.680325	-0.680325	-0.677057	-0.677057	-0.677057	1.119998×10^{-7}	1.119998×10^{-7}
0.5	0.0	-1.121670	-1.121670	-1.116280	-1.116280	-1.116280	1.846565×10^{-7}	1.846565×10^{-7}
	0.5	-1.849320	-1.849320	-1.840430	-1.840430	-1.840430	3.044472×10^{-7}	3.044472×10^{-7}
	1.0	-3.049010	-3.049010	-3.034360	-3.034360	-3.034360	5.019485×10^{-7}	5.019485×10^{-7}
	-1.	-0.4158180	-0.415818	-0.414782	-0.414782	-0.414783	5.448142×10^{-7}	5.448142×10^{-7}
	-0.5	-0.685568	-0.685568	-0.683861	-0.683861	-0.683861	8.982467×10^{-7}	8.982467×10^{-7}
1.0	0.0	-1.130310	-1.130310	-1.127500	-1.127500	-1.127500	1.480958×10^{-6}	1.480958×10^{-6}
	0.5	-1.863570	-1.863570	-1.858930	-1.858930	-1.858930	2.441687×10^{-6}	2.441687×10^{-6}
	1.0	-3.072500	-3.072500	-3.064850	-3.064850	-3.064850	4.025662×10^{-6}	4.025662×10^{-6}

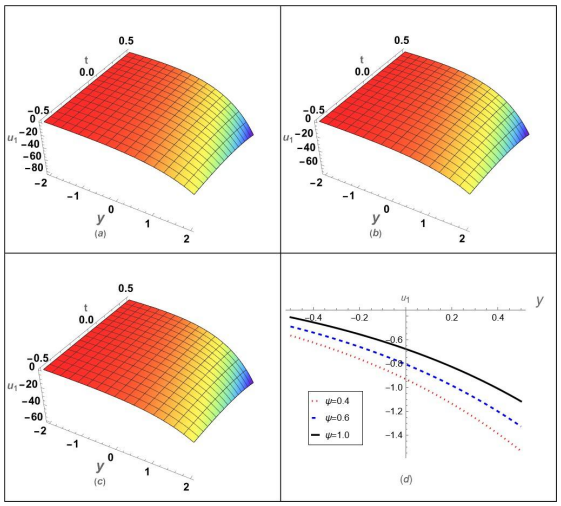


Figure 1: Effect of fractional order, (a) $\psi = 0.4$, (b) $\psi = 0.6$, (c) $\psi = 1.0$ on the approximate solution and (d) comparison of fractional order ψ of the solution $u_1(y,z,t)$ at $t = 1$, $\hbar = -1$, and $z = 0.1$.

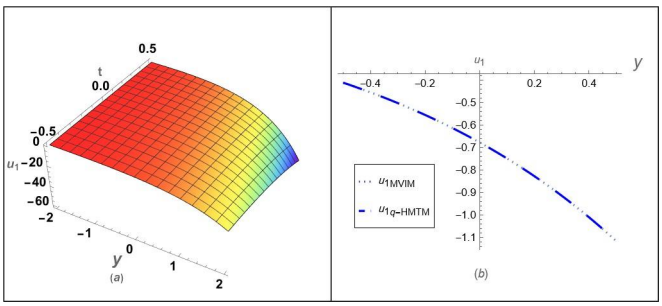


Figure 2: Comparison among MVIM and q-HMTM solution $u_1(y, z, t)$ at $t = 1$, $\hbar = -1$, and $z = 0.1$.

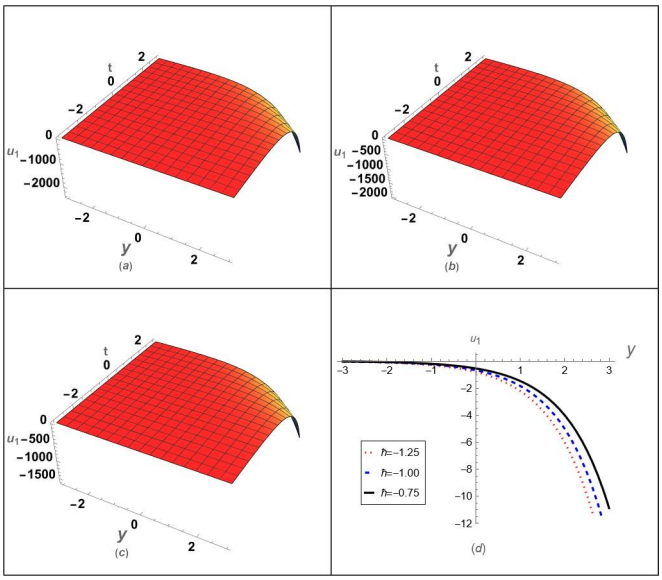


Figure 3: Effect of the auxiliary parameter, (a) $\hbar t = -1.25$, (b) $\hbar = -1$, (c) $\hbar = -0.75$ on the approximate solution $u_1(y, z, t)$ at $= 1$ and $z = 0.1$.

Table 2: q-HMTM and MVIM solution error comparison of $u_2(y, z, t)$ at $z = 0.1$ and $\hbar = -1$.

t	y	$\text{MVIM}_{\psi=0.6}$	$\text{q-HMTM}_{\psi=0.6}$	$\text{MVIM}_{\psi=1}$	$\text{q-HMTM}_{\psi=1}$	Exact	$\text{MVIM Error}_{\psi=1}$	$\text{q-HMTM Error}_{\psi=1}$
	-1.0	0.408865	0.408865	0.407384	0.407384	0.407384	5.423639×10^{-10}	5.423640×10^{-10}
	-0.5	0.674104	0.674104	0.671662	0.671662	0.671662	8.942070×10^{-10}	8.942071×10^{-10}
0.1	0.0	1.111410	1.111410	1.107380	1.107380	1.107380	1.474298×10^{-9}	1.474298×10^{-9}
	0.5	1.832410	1.832410	1.825770	1.825770	1.825770	2.430706×10^{-9}	2.430706×10^{-9}
	1.0	3.021130	3.021130	3.010180	3.010180	3.010180	4.007557×10^{-9}	4.007558×10^{-9}
	-1.0	0.412638	0.412638	0.410656	0.410656	0.410656	6.793135×10^{-8}	6.793135×10^{-8}
	-0.5	0.680325	0.680325	0.677057	0.677057	0.677057	1.119998×10^{-7}	1.119998×10^{-7}
0.5	0.0	1.121670	1.121670	1.116280	1.116280	1.116280	1.846565×10^{-7}	1.846565×10^{-7}
	0.5	1.849320	1.849320	1.840430	1.840430	1.840430	3.044472×10^{-7}	3.044472×10^{-7}
	1.0	3.049010	3.049010	3.034360	3.034360	3.034360	5.019485×10^{-7}	5.019485×10^{-7}
	-1.	0.4158180	0.415818	0.414782	0.414782	0.414783	5.448142×10^{-7}	5.448142×10^{-7}
	-0.5	0.685568	0.685568	0.683861	0.683861	0.683861	8.982467×10^{-7}	8.982467×10^{-7}
1.0	0.0	1.130310	1.130310	1.127500	1.127500	1.127500	1.480958×10^{-6}	1.480958×10^{-6}
	0.5	1.863570	1.863570	1.858930	1.858930	1.858930	2.441687×10^{-6}	2.441687×10^{-6}
	1.0	3.072500	3.072500	3.064850	3.064850	3.064850	4.025662×10^{-6}	4.025662×10^{-6}

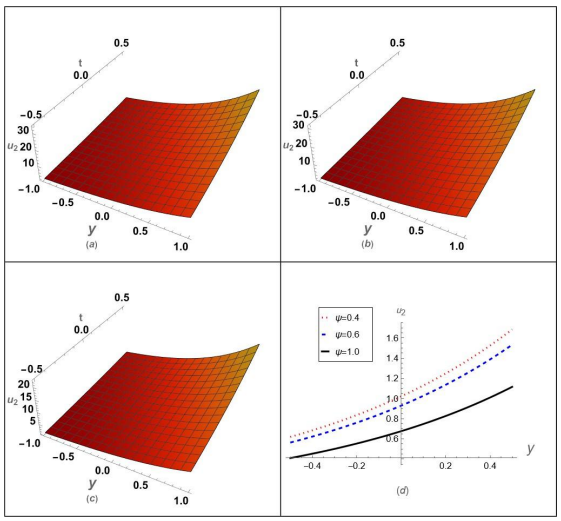


Figure 4: Effect of fractional order, (a) $\psi = 0.4$, (b) $\psi = 0.6$, (c) $\psi = 1.0$ on the approximate solution and (d) comparison of fractional order ψ of the solution $u_2(y, z, t)$ at $t = 1$, $\hbar = -1$, and $z = 0.1$.

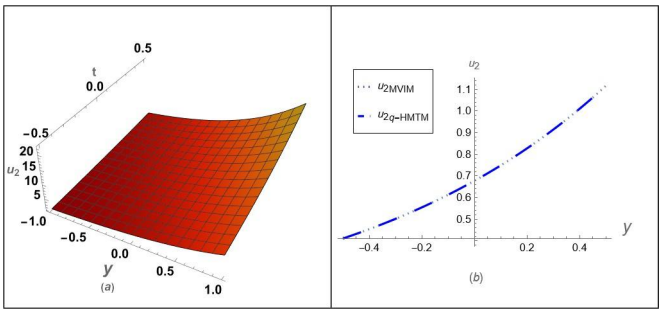


Figure 5: Comparison among MVIM solution and q-HMTM solution $u_2(y, z, t)$ at $t = 1$, $\hbar = -1$, and $z = 0.1$.

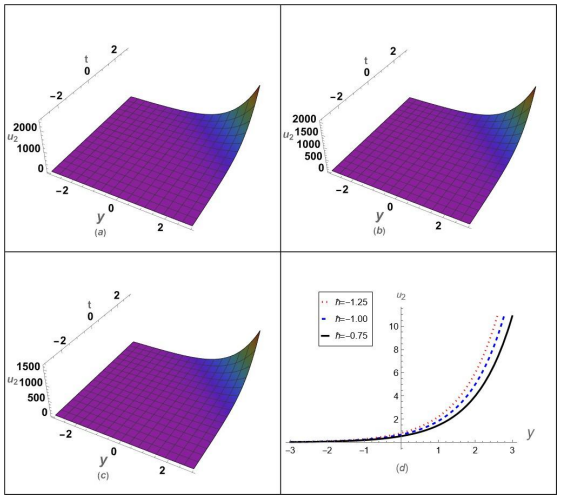


Figure 6: Effect of the auxiliary parameter, (a) $\hbar t = -1.25$; (b) $\hbar = -1$; (c) $\hbar = -0.75$ on the approximate solution $u_2(y, z, t)$ at $= 1$ and $z = 0.1$.

4. Numerical example 2

4.1. *Utilization of* q-*HMTM*

Assume the NS equation of time fractional order:

$$D_t u_1 - a\left(\frac{\partial^2 u_1}{\partial y^2} + \frac{\partial^2 u_1}{\partial z^2}\right) + u_2 \frac{\partial u_1}{\partial z} + u_1^{\psi} \frac{\partial u_1}{\partial y} - q = 0,$$

$$D_t^{\psi} u_2 - a\left(\frac{\partial^2 u_2}{\partial y^2} + \frac{\partial^2 u_2}{\partial z^2}\right) + u_1 \frac{\partial u_2}{\partial y} + u_2 \frac{\partial u_2}{\partial z} + q = 0, \tag{5.1}$$

where $0 < \psi \leqslant 1$. IC's are given as:

$$u_1(y, z, 0) = -\sin(y+z),$$
$$u_2(y, z, 0) = \sin(y+z),$$

$$\frac{1}{s^\psi} M\left[u_1 - s\left(\sin(y+z)\right) + \hbar\left(-a\frac{\partial^2 u_1}{\partial y^2} - a\frac{\partial^2 u_1}{\partial z^2} + u_2\frac{\partial u_1}{\partial z} + u_1\frac{\partial u_1}{\partial y} - q\right)\right] = 0,$$

$$\frac{1}{s^\psi} M\left[u_2 + s\left(\sin(y+z)\right) + \hbar\left(-a\frac{\partial^2 u_2}{\partial y^2} - a\frac{\partial^2 u_2}{\partial z^2} \pm u_1\frac{\partial u_2}{\partial y} + u_2\frac{\partial u_2}{\partial z} + q\right)\right] = 0.$$

The non-linear operator is defined as:

$$\begin{aligned} &N^1[\varphi_1(y, z, t; q), \varphi_2(y, z, t; q)] \\ &= M[\varphi_1(y, z, t; q)] - s\left(\sin(y+z)\right) + \frac{1}{s^\psi} M\left[\hbar\left(-a\frac{\partial^2 \varphi_1(y, z, t; q)}{\partial y^2}\right.\right. \\ &\left.\left. - a\frac{\partial^2 \varphi_1(y, z, t; q)}{\partial z^2} + \varphi_2(y, z, t; q)\frac{\partial \varphi_1(y, z, t; q)}{\partial z} + \varphi_1(y, z, t; q)\frac{\partial \varphi_1(y, z, t; q)}{\partial y} - q\right)\right], \\ &N^2[\varphi_1(y, z, t; q), \varphi_2(y, z, t; q)] \\ &= M[\phi_2(y, z, t; q)] + s\left(\sin(y+z)\right) + \frac{1}{s^\psi} M\left[\hbar\left(-a\frac{\partial^2 \varphi_2(y, z, t; q)}{\partial y^2}\right.\right. \\ &\left.\left. - a\frac{\partial^2 \varphi_2(y, z, t; q)}{\partial z^2} + \varphi_1(y, z, t; q)\frac{\partial \varphi_2(y, z, t; q)}{\partial y} + \varphi_2(y, z, t; q)\frac{\partial \varphi_2(y, z, t; q)}{\partial z} + q\right)\right]. \end{aligned}$$

The Mohand operator is defined as:

$$M[u_{1m} - k_m u_{1m-1}] = \hbar\, h(y, z, t) R_{1,m}[\vec{u}_{1m-1}, \vec{u}_{2m-1}],$$
$$M[u_{2m} - k_m u_{2m-1}] = \hbar\, h(y, z, t) R_{2,m}[\vec{u}_{1m-1}, \vec{u}_{2m-1}].$$

Here,

$$\begin{aligned} &R_{1,m}[\vec{u}_{1m-1}, \vec{u}_{2m-1}] \\ &= M[u_{1m-1}] - k_m s\left(1 - \frac{1}{n_{m-1}}\right)\left(\sin(y+z)\right) + \frac{1}{s^\psi} M\left[\hbar\left(-a\frac{\partial^2 u_{1m-1}}{\partial y^2}\right.\right. \\ &\left.\left. - a\frac{\partial^2 u_{1m-1}}{\partial z^2} + \sum_{i=0}^{n_{m-1}} u_{2i}\frac{\partial u_{1m-1-i}}{\partial z} + \sum_{i=0}^{n_{m-1}} u_{1i}\frac{\partial u_{1m-1-i}}{\partial y} - q\right)\right], \\ &R_{2,m}[\vec{u}_{1m-1}, \vec{u}_{2m-1}] \\ &= M[u_{2m-1}] + k_m s\left(1 - \frac{1}{n_{m-1}}\right)\left(\sin(y+z)\right) + \frac{1}{s^\psi} M\left[\hbar\left(-a\frac{\partial^2 u_{2m-1}}{\partial y^2}\right.\right. \\ &\left.\left. - a\frac{\partial^2 u_{2m-1}}{\partial z^2} + \sum_{i=0}^{n_{m-1}} u_{1i}\frac{\partial u_{2m-1-i}}{\partial y} + \sum_{i=0}^{n_{m-1}} u_{2i}\frac{\partial u_{2m-1-i}}{\partial z} + q\right)\right], \end{aligned}$$

$$u_{1m} = k_m u_{1m-1} + \hbar M^{-1}[h(y, z, t) R_{1,m}(\vec{u}_{1m-1}, \vec{u}_{2m-1}), \quad (5.2)$$
$$u_{2m} = k_m u_{2m-1} + \hbar M^{-1}[h(y, z, t) R_{2,m}(\vec{u}_{1m-1}, \vec{u}_{2m-1}).$$

With the help of initial condition (5.2) we obtain the subsequent outcome:

$$u_{11} = \frac{\hbar t^\psi(-2a\sin(y+z) - q)}{\Gamma(\psi+1)},$$

$$u_{21} = \frac{\hbar t^{\psi}(2a\sin(y+z)+q)}{\Gamma(\psi+1)},$$

$$u_{12} = \hbar t^{\psi} - \frac{4a^2\hbar t^{\psi}\sin(y+z)}{\Gamma(2\psi+1)} - \frac{(n+\hbar)(2a\sin(y+z)+q)}{\Gamma(\psi+1)},$$

$$u_{22} = \hbar t^{\psi}\frac{(n+\hbar)(2a\sin(y+z)+q)}{\Gamma(2\psi+1)} + \frac{4a^2\hbar t^{\psi}\sin(y+z)}{\Gamma(\psi+1)},$$

and so on. The solution of equation (5.1), as determined by q-HMTM, is as follows:

$$u_1 = u_{10} + \sum_{m=1}^{\infty} u_{1m}\left(\frac{1}{n}\right)^m, \quad u_2 = u_{20} + \sum_{m=1}^{\infty} u_{2m}\left(\frac{1}{n}\right)^m.$$

For $\psi = 1$, $\hbar = -1$, and $n = 1$ solutions $\sum_{m=1}^{N} u_{1m}\left(\frac{1}{n}\right)^m$ and $\sum_{m=1}^{N} u_{2m}\left(\frac{1}{n}\right)^m$ converge to the exact solutions as $N \to \infty$,

$$u_1(y,z,t) = -\sin(y+z) + \frac{\hbar t^{\psi}(-2a\sin(y+z)-q)\,\Gamma(\psi+1)}{} + \hbar t^{\psi} - \frac{4a^2\hbar t^{\psi}\sin(y+z)}{\Gamma(2\psi+1)} - \frac{(n+\hbar)(2a\sin(y+z)+q)}{\Gamma(\psi+1)} = -e^{-2at}\sin(y+z),$$

$$u_2(y,z,t) = \sin(y+z) + \frac{\hbar t^{\psi}(2a\sin(y+z)+q)\,\Gamma(\psi+1)}{} + \hbar t^{\psi} - \frac{4a^2\hbar t^{\psi}\sin(y+z)}{\Gamma(2\psi+1)} + \frac{(n+\hbar)(2a\sin(y+z)+q)}{\Gamma(\psi+1)} = e^{-2at}\sin(y+z).$$

4.2. Utilization of MVIM

Assume the NS equation of time fractional order:

$$D_t^{\psi} u_1 = a\frac{\partial^2 u_1}{\partial y^2} + a\frac{\partial^2 u_1}{\partial z^2} - u_2\frac{\partial u_1}{\partial z} - u_1\frac{\partial u_1}{\partial y} - q, \qquad D_t^{\psi} u_2 = a\frac{\partial^2 u_2}{\partial y^2} + a\frac{\partial^2 u_2}{\partial z^2} - u_1\frac{\partial u_2}{\partial y} - u_2\frac{\partial u_2}{\partial z} + q, \tag{5.3}$$

where $0 < \psi \leqslant 1$. IC's are given as $u_1(y,z,0) = -\sin(y+z)$, $u_2(y,z,0) = \sin(y+z)$. Using the iterative formula found in equation (3.9), we can obtain

$$u_{1n+1} = u_{1n} + M\left[\frac{\hbar}{s^{\psi}}\right]^{-1}\left[\sum_{k=0}^{n-1} s^{\psi-k-1}\frac{\partial^k u_1(y,z,0)}{\partial t^k} + M\left[a\frac{\partial^2 u_{1n}}{\partial y^2} + a\frac{\partial^2 u_{1n}}{\partial z^2} - u_{2n}\frac{\partial u_{1n}}{\partial z} - u_1\frac{\partial u_{1n}}{\partial y} - q\right]\right],$$

$$u_{2n+1} = u_{2n} + M\left[\frac{\hbar}{s^{\psi}}\right]^{-1}\left[\sum_{k=0}^{n-1} s^{\psi-k-1}\frac{\partial^k u_2(y,z,0)}{\partial t^k} + M\left[a\frac{\partial^2 u_{2n}}{\partial y^2} + a\frac{\partial^2 u_{2n}}{\partial z^2} - u_{1n}\frac{\partial u_{2n}}{\partial y} - u_2\frac{\partial u_{2n}}{\partial z} + q\right]\right].$$

Inserting $n = 0$ into the expression above results in the second approximation we have

$$u_{11} = u_{10} + M\left[\frac{\hbar}{s^{\psi}}\right]^{-1}\left[\sum_{k=0}^{n-1} s^{\psi-k-1}\frac{\partial^k u_1(y,z,0)}{\partial t^k} + M\left[a\frac{\partial^2 u_{10}}{\partial y^2} + a\frac{\partial^2 u_{10}}{\partial z^2} - u_{20}\frac{\partial u_{10}}{\partial z} - u_{10}\frac{\partial u_{10}}{\partial y} - q\right]\right],$$

$$u_{21} = u_{20} + M\left[\frac{\hbar}{s^{\psi}}\right]^{-1}\left[\sum_{k=0}^{n-1} s^{\psi-k-1}\frac{\partial^k u_2(y,z,0)}{\partial t^k} + M\left[a\frac{\partial^2 u_{20}}{\partial y^2} + a\frac{\partial^2 u_{20}}{\partial z^2} - u_{10}\frac{\partial u_{20}}{\partial y} - u_{20}\frac{\partial u_{20}}{\partial z} + q\right]\right].$$

By simplification, we get

$$u_{11} = \frac{\sin(y+z)\,2at^{\psi} - \Gamma(\psi+1) + qt^{\psi}}{\Gamma(\psi+1)}, \quad u_{21} = \frac{\sin(y+z)\,\Gamma(\psi+1) - 2at^{\psi} - qt^{\psi}}{\Gamma(\psi+1)}$$

By taking n = 1, we have

$$u_{12} = u_{11} + M\,u_{22-1}^{-1}\left[\frac{1}{s^{\psi}}\sum_{k=0}^{n-1} s^{\psi-k-1}\frac{\partial^k u_1(y,z,0)}{\partial t^k} + M\left[a\frac{\partial^2 u_{11}}{\partial y^2} + a\frac{\partial^2 u_{11}}{\partial z^2} - u_{21}\frac{\partial u_{11}}{\partial z} - u_{11}\frac{\partial u_{11}}{\partial y} - q\right]\right],$$

$$= u_{21} + M\,{}_{-1}^{-1}\left[\frac{1}{s^{\psi}}\sum_{k=0}^{n-1} s^{\psi-k-1}\frac{\partial^k u_2(y,z,0)}{\partial t^k} + M\left[a\frac{\partial^2 u_{21}}{\partial y^2} + a\frac{\partial^2 u_{21}}{\partial z^2} - u_{11}\frac{\partial u_{21}}{\partial y} - u_{21}\frac{\partial u_{21}}{\partial z} + q\right]\right].$$

By simplifying the expression, we achieve the subsequent final outcome.

$$u_{12}(y,z,t) = -\sin(y+z) + \frac{2at^{\psi}\sin(y+z)}{\Gamma(\psi+1)} + \frac{qt^{\psi}}{\Gamma(\psi+1)} - \frac{4a^2t^{2\psi}\sin(y+z)}{\Gamma(2\psi+1)}$$

$$u_{22}(y,z,t) = \sin(y+z) - \frac{2at^{\psi}\sin(y+z)}{\Gamma(\psi+1)} - \frac{qt^{\psi}}{\Gamma(\psi+1)} + \frac{4a^2t^{2\psi}\sin(y+z)}{\Gamma(2\psi+1)}$$

Table 3: q-HMTM and MVIM solution error comparison of $u_1(y,z,t)$ at $z = 0.1$ and $\hbar = -1$.

t	y	MVIM$_{\psi=0.6}$	q-HMTM$_{\psi=0.6}$	MVIM$_{\psi=1}$	q-HMTM$_{\psi=1}$	Exact	MVIM Error$_{\psi=1}$	q-HMTM Error$_{\psi=1}$
	-1.0	0.778941	0.778941	0.781762	0.781762	0.781762	1.043913×10^{-9}	1.043913×10^{-9}
	-0.5	0.387238	0.387238	0.388640	0.388640	0.388640	5.189649×10^{-10}	5.189649×10^{-10}
0.1	0.0	-0.099274	-0.099274	-0.099633	-0.099633	-0.099633	1.330447×10^{-10}	1.330446×10^{-10}
	0.5	-0.561481	-0.561481	-0.563514	-0.563514	-0.563514	7.524804×10^{-10}	7.524803×10^{-10}
	1.0	-0.886217	-0.886217	-0.889427	-0.889427	-0.889427	1.187682×10^{-9}	1.187682×10^{-9}
	-1.0	0.771883	0.771883	0.775533	0.775533	0.775533	1.302287×10^{-7}	1.302287×10^{-7}
	-0.5	0.383729	0.383729	0.385544	0.385544	0.385544	6.474112×10^{-8}	6.474112×10^{-8}
0.5	0.0	-0.098374	-0.098374	-0.098840	-0.098840	-0.098840	1.659738×10^{-8}	1.659738×10^{-8}
	0.5	-0.556393	-0.556393	-0.559024	-0.559024	-0.559024	9.387228×10^{-8}	9.387228×10^{-8}
	1.0	-0.878187	-0.878187	-0.882340	-0.882340	-0.882340	1.481639×10^{-7}	1.481639×10^{-7}
	-1.0	0.766078	0.7660780	0.767817	0.767817	0.767816	1.039234×10^{-6}	1.039234×10^{-6}
	-0.5	0.380843	0.3808430	0.381708	0.381708	0.381707	5.166386×10^{-7}	5.166386×10^{-7}
1.0	0.0	-0.097635	-0.097635	-0.097856	-0.097856	-0.097856	1.324483×10^{-7}	1.324483×10^{-7}
	0.5	-0.552209	-0.552209	-0.553463	-0.553463	-0.553462	7.491073×10^{-7}	7.491073×10^{-7}
	1.0	-0.871583	-0.871583	-0.873561	-0.873561	-0.873560	1.182358×10^{-6}	1.182358×10^{-6}

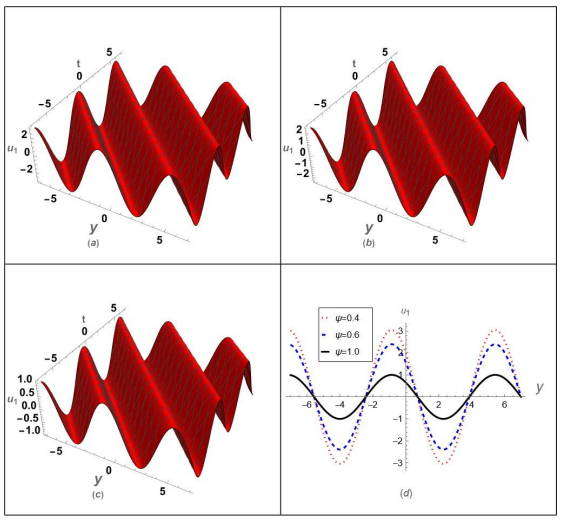


Figure 7: Effect of fractional order, (a) $\psi = 0.4$; (b) $\psi = 0.6$; (c) $\psi = 1.0$ on the approximate solution; and (d) comparison of fractional order ψ of the solution $u_1(y,z,t)$ at $t = 1$, $\hbar = -1$, and $z = 0.1$.

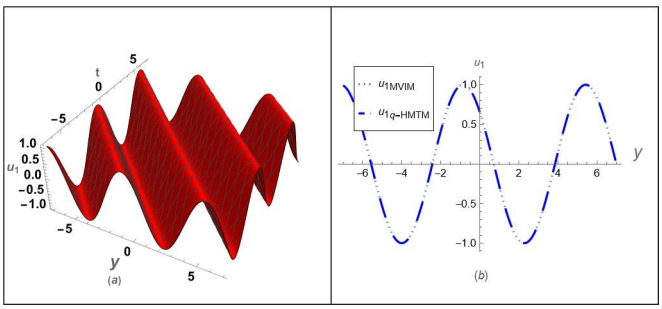


Figure 8: Comparison among MVIM and q-HMTM solution $u_1(y, z, t)$ at $t = 1$, $\hbar = -1$, and $z = 0.1$.

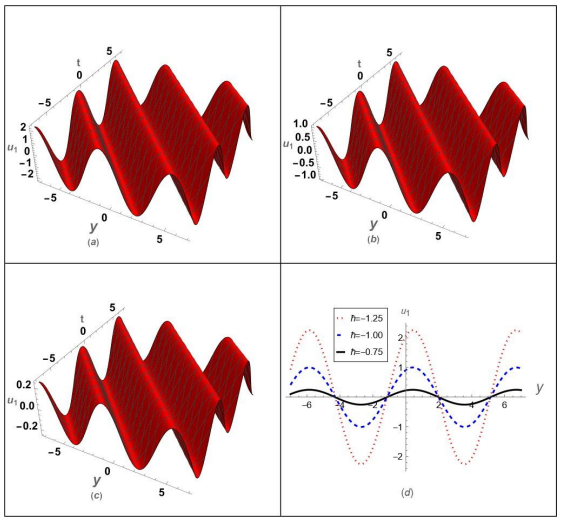


Figure 9: Effect of the auxiliary parameter, (a) $\hbar t = -1.25$; (b) $\hbar = -1$; (c) $\hbar = -0.75$ on the approximate solution $u_1(y, z, t)$ at $= 1$ and $z = 0.1$.

Table 4: q-HMTM and MVIM solution error comparison of $u_2(y, z, t)$ at $z = 0.1$ and $\hbar = -1$.

t	y	$MVIM_{\psi=0.6}$	$q\text{-}HMTM_{\psi=0.6}$	$MVIM_{\psi=1}$	$q\text{-}HMTM_{\psi=1}$	Exact	$MVIM\ Error_{\psi=1}$	$q\text{-}HMTM\ Error_{\psi=1}$
-1.0		-0.778941	-0.778941	-0.781762	-0.781762	-0.781762	1.043913×10^{-9}	1.043913×10^{-9}
-0.5		-0.387238	-0.387238	-0.388640	-0.388640	-0.388640	5.189649×10^{-10}	5.189649×10^{-10}
0.1	0.0	0.099274	0.099274	0.099633	0.099633	0.099633	1.330446×10^{-10}	1.330446×10^{-10}
0.5		0.561481	0.561481	0.563514	0.563514	0.563514	7.524803×10^{-10}	7.524803×10^{-10}
1.0		0.886217	0.886217	0.889427	0.889427	0.889427	1.187682×10^{-9}	1.187682×10^{-9}
-1.0		-0.771883	-0.771883	-0.775533	-0.775533	-0.775533	1.302287×10^{-7}	1.302287×10^{-7}
-0.5		-0.383729	-0.383729	-0.385544	-0.385544	-0.385544	6.474112×10^{-8}	6.474112×10^{-8}
0.5	0.0	0.098374	0.098374	0.098840	0.098840	0.098840	1.659738×10^{-8}	1.659738×10^{-8}
0.5		0.556393	0.556393	0.559024	0.559024	0.559024	9.387228×10^{-8}	9.387228×10^{-8}
1.0		0.878187	0.878187	0.882340	0.882340	0.882340	1.481639×10^{-7}	1.481639×10^{-7}
-1.0		-0.766078	-0.766078	-0.767817	-0.767817	-0.767816	1.039234×10^{-6}	1.039234×10^{-6}
-0.5		-0.380843	-0.380843	-0.381708	-0.381708	-0.381707	5.166386×10^{-7}	5.166386×10^{-7}
1.0	0.0	0.097635	0.097635	0.097856	0.097856	0.097856	1.324483×10^{-7}	1.324483×10^{-7}
0.5		0.552209	0.552209	0.553463	0.553463	0.553462	7.491073×10^{-7}	7.491073×10^{-7}
1.0		0.871583	0.871583	0.873561	0.873561	0.873560	1.182358×10^{-6}	1.182358×10^{-6}

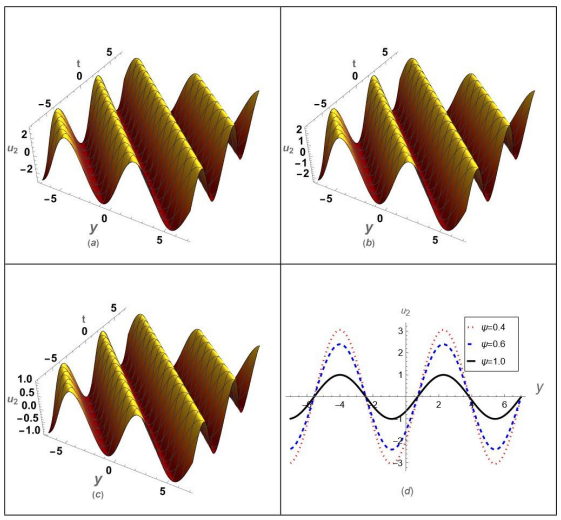


Figure 10: Effect of fractional order, (a) $\psi = 0.4$; (b) $\psi = 0.6$; (c) $\psi = 1.0$ on the approximate solution; and (d) comparison of fractional order ψ of the solution $u_2(y, z, t)$ at $t = 1$, $\hbar = -1$, and $z = 0.1$.

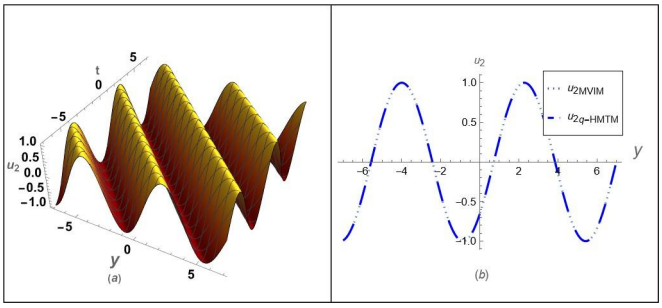


Figure 11: Comparison among MVIM solution and q-HMTM solution $u_2(y, z, t)$ at $t = 1$, $\hbar = -1$, and $z = 0.1$.

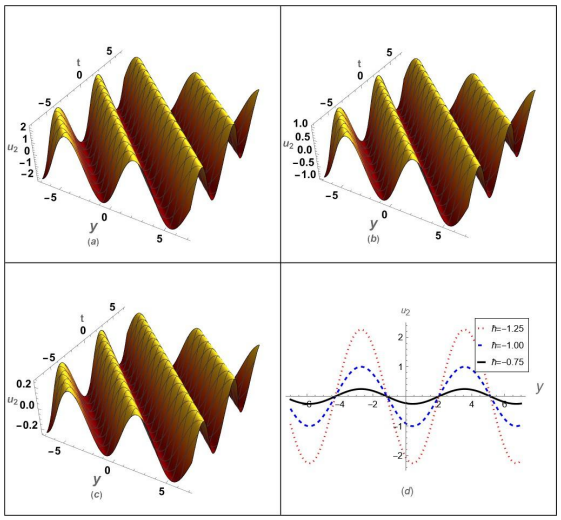


Figure 12: Effect of the auxiliary parameter, (a) $\hbar t = -1.25$; (b) $\hbar = -1$; (c) $\hbar = -0.75$ on the approximate solution $u_2(y, z, t)$ at $= 1$ and $z = 0.1$.

5. Result and discussion

The numerical studies illustrated in Tables 1-4 and Figures 1-11 form a thorough comparison between the two methods, the MVIM, and the q-HMTM in solving the time-fractional NS equations under two different sets of initial conditions. Both methods are very accurate in all the test cases, it is clear that the absolute errors are extremely small. This proves both approaches to be efficient and reliable in solving

problems of fractional fluid dynamics.

The numerical result of u_1 and u_2 determined using MVIM and q-HMTM in the case of Problem 1 are given in the Tables 1-2 are quite near to the exact solution. The absolute errors in the case of $\psi = 1$ are small at all-time levels, which means that the approximation is numerically stable and quite precise. Referring to Figures 1 and 4 we noticed that the profiles of the solutions are highly affected by the fractional order ψ in the sense that as ψ deviates and moves from the value of 0.4 to 1.0, the solutions start showing reduction in memory effect and converging to their classical integer-order counterparts. This fact is further indicated by the dominance of the time curves generated by MVIM and q-HMTM shown in Figures 2 and 5, which are approximately same, expressing the harmony of the two methods.

Similarly for Problem 2 the values of u_1 and u_2 determined using MVIM and q-HMTM are given in the Tables 3-4, in this case the sinusoidal initial conditions are used. Absolute errors of the two methods are both in the negligible level and have close concurrence with the exact solutions. In Figures 7 and 10, the obvious role of the fractional order is once more demonstrated: the lower ψ lead to the slower diffusion and more oscillatory dynamics, whereas $\psi = 1$ results in smoother profiles that resemble NS dynamics. Comparisons in Figures 8 and 11 prove that q-HMTM is slightly faster in converging without affecting numerical stability in comparison with MVIM.

The auxiliary parameter $\hbar$ is very important in regulating convergence and accuracy of approximate solutions to q-HMTM. The effect of varying values of $\hbar$ (i.e., $\hbar$= -0.75,-1,-1.25) on solutions u_1 and u_2 at $t = 1$ and $z = 0.1$ is clearly shown in Figures 3, 6, 9, and 12. The difference between the curves of the solutions is noted to be altered by changing the auxiliary parameter in terms of shape and amplitude. As an example, by setting $\hbar = -1.25$, the solution will have some greater deviations whereas $\hbar = -0.75$ will have smoother curves. The case $\hbar = -1$ seems to provide a more symmetric and stable profile and better convergence properties and compatibility with the expected results of the fractional-order NS system. This also shows that $\hbar$ can be viewed as convergence-control parameter where one can be flexible to modify the approximation based on the kind of nonlinear fractional model of interest. Reasonable choice of $\hbar$ is thus key to resolving correct and stable solutions, and the given graphical data explains that the given q-HMTM indeed offers a successful platform to make such adjustment.

The results also highlight the physical significance of fractional-order effects in fluid dynamics. Varia- tions in ψ directly influence the evolution of the flow field: smaller values of ψ enhance memory effects, leading to slower decay of vorticity and more sustained flow structures, while larger values reduce these effects, approaching the behavior of the classical NS model. This adaptability allows the fractional-order NS equations to model a wider spectrum of fluid phenomena, including anomalous diffusion in porous media and the complex decay behavior in viscoelastic or turbulent flows. The combined application of the Mohand transformation, with its computational advantages over other transforms, and the convergence control offered by $\hbar = -1$ in the q-HMTM framework therefore provides a powerful and precise approach for exploring such fractional-order fluid systems.

6. Conclusion

In this research, MVIM and q-HMTM were successfully used to solve the time-fractional NS equations. In order to demonstrate that both approaches provide exceptional accuracy and low mistakes even in the case of nonlinear coupled systems, these conclusions were confirmed using precisely defined solutions. The Mohand transformation, q-HAM, and VIM framework worked well together to preserve the non-trivial memory effects that fractional-order models display while also producing much quicker convergence and stability. When compared to alternative techniques of fractional operator translation, particularly with regard to multi-term fractional operators, the Mohand transformation also demonstrated to be more straightforward, effective, and reliable in terms of computing benefit. Furthermore, the behavior of the fluid is sufficiently flexible to describe both the standard and anomalous transport processes, as shown by the dependency of the fractional order ψ. In general, the Mohand transformation in conjunction with q-HAM and VIM provides a reliable and elegantly succinct approach to conducting precise and accurate analytical studies of intricate fractional fluid dynamics processes. This suggests that there will be opportunities in the future to investigate advanced fluid dynamics as well as in real-world applications.

References

[1] AIP Conf. Proc., 1940 (2018), 1–6. S. Abuasad, I. Hashim, Homotopy decomposition approach for solving one-dimensional time-fractional diffusion equation
[2] S. Abuasad, I. Hashim, Homotopy decomposition approach for using modified beta derivative to solve higher-order time-fractional diffusion equation, Sains Malays, 47 (2018), 2899–2905. 1

[3] J. F. Gomez-Aguilar, S. Abuasad, A. Yildirim, I. Hashim, S. A. Abdul Karim, A technique for approximating a fractional stochastic SIS epidemic model with imperfect vaccination using fractional multi-step differential transformation, Int. J. Environ. Res. Public Health, 16 (2019), 15 pages. 1 [4] J. Adams, L. Wright, R. Parker, W. Harris, G. Jenkins, A comparative analysis of Mohand and Elzaki transforms, 15 (2024), 17–26. One
[5] G. Adomian, The decomposition approach for solving physics frontier issues, Kluwer Academic Publishers Group, Dordrecht, 1994. One
[6] A comparison of Mohand and Laplace transforms by S. Aggarwal and R. Chaudhary, J. Emerg. Technol. Innov. Res., 6 (2019), 230–240. 1 [7] A comparison of the Mohand and Aboodh transforms, S. Aggarwal, R. Chauhan, Int. J. Res. Advent Technol., 7 (2019), 520–529.
[8] S. Aggarwal, A. R. Gupta, Mohand transform duality and some practical integral transforms, Int. J. Recent Technol. Eng., 8 (2019), 843–847.
[9] A comparative analysis of Mohand and Sumudu transforms, S. Aggarwal and S. D. Sharma, J. Emerg. Technol. Innov. Res., 6 (2019), 145–153. 1 [10] K. Nonlaopon, S. Aly, R. Shah, N. A. Shah, A. A. Alderremy, Two updated analytical methods for time fractional partial differential equation systems are compared, AIMS Math., 8 (2023), 7142–7162. One
[11] J.-H. He, N. Anjum, Laplace transform: simplifying the variational iteration approach, Appl. Math. Lett., 92 (2019), 134–138. One
[12] D. Baleanu, J. A. Tenreiro Machado, Z. B. Güvenç, Applications of fractional calculus to emerging developments in nanotechnology, Springer, New York, 2010). One
[13]D. Baleanu, G.-C. Wu, and S.-D. Zeng, extended Caputo fractional differential equations: Chaos analysis and asymptotic stability, Chaos Solitons Fractals, 102 (2017), 99–105. One
[14] G. A. Birajdar, Discrete Adomian decomposition approach for numerical solution of time-fractional Navier-Stokes equation, Nonlinear Eng., 3 (2014), 21–26. A. Bokhari, "Shehu transform applied to Atangana-Baleanu derivatives," Journal of Mathematical Computing Science, 20 (2019), 101–107. 1 [16] H. Bulut, M. Eslami, M. Mirzazadeh, T. A. Sulaiman, H. M. Baskonus, H. Rezazadeh, Optical solitons and alternative solutions to the fractional Fokas-Lenells equation in conformable space-time, Optik, 172 (2018), 20–27. 1 [17] V. B. L. Chaurasia, D. Kumar, Navier-Stokes equation solution for temporal fractions, Gen. Math. Notes, 4 (2011), 49–59.
1 [18] M. Dehghan, Finite difference methods for resolving issues that come up during the design and modeling of specific optoelectronic devices, 16–30 in Math. Comput. Simul., 71 (2006). 1 [19] A. Salem, M. El-Shahed, Regarding the Navier-Stokes equations in general, 287–293 in Appl. Math. Comput., 156 (2004). 1 [20] Z. Z. Ganji, D. D. Ganji, A. D. Ganji, M. Rostamian, Time-fractional Navier-Stokes equation analytically solved in polar coordinates using the homotopy perturbation approach, Numer. Methods Partial Differ. Equ., 26 (2010), 117–124. Comput. Methods Appl. Mech. Eng., 167 (1998), 69–73; 1 [21]J. H. He, Approximate solution of nonlinear differential equations using convolution product nonlinearities. Appl. Math. Comput., 114 (2000), 115–123; 1 [22] J.-H. He, Variational iteration approach for autonomous ordinary differential systems. Fractional calculus: an introduction for physicists, R. Herrmann, World Scientific, Singapore, 2011 [23]. 1 [24] R. Hilfer, Fractional calculus applications in physics, World Scientific, Singapore (2000). One
[25]J. Adv. Res., 32 (2021), 133–138. 2.4 H. Jafari, A novel generic integral transform for solving integral equations

[26] A. Kadem, A. Khalouta, Inverse fractional Shehu transform method: a novel approach to fractional differential equations, Appl. Appl. Math., 14 (2019), 926–941. One

[27] A. A. Kilbas, J. J. Trujillo, H. M. Srivastava, Fractional differential equation theory and applications, Elsevier Science B.V., Amsterdam, 2006). One
[28]S. Abbasbandy, D. Kumar, M. M. Rashidi, S. Kumar, The fractional Navier-Stokes equation may be solved analytically using the modified Laplace decomposition technique. Ain Shams Engineering Journal, 5 (2014), 569–574. One
[29]J. Singh, S. Kumar, D. Kumar, A fractional model of the Navier-Stokes equation that arises in viscous fluid flow that is not stable, J. Assoc. Arab Univ. Basic Appl. Sci., 17 (2015), 14–19. 1 [30] Adapted homotopy perturbation approach with Shehu transform for solving conformable fractional nonlinear partial differential equations, Fractals, 31 (2023), 19 pages, M. I. Liaqat, A. Khan, M. A. Alqudah, and T. Abdeljawad. One
[31] J. Liouville, Second memoir on the development of functions or groups of functions in series when the various terms are assumed to satisfy a second-order differential equation with a variable parameter, J. Math. Pure et Appl., 2 (1837), 16–35. 1 [32] Millimeter-wave E-plane waveguide bandpass filters based on spoof surface plasmon polaritons, IEEE Trans. Microw. Theory Tech., 70 (2022), 4399–4409, Y. Liu, K. D. Xu, J. Li, Y. J. Guo, A. Zhang, Q. Chen. One
[33] D. Xin, C. Sun, G. Gao, G. Wu, B. Gao, Z. Yang, W. Wei, and K. Liu High Voltage, 8 (2023), 358–367, "Novel detection approach for thermal defects: Study on its feasibility and application to vehicle cables." One
[34] L. Liu, L. Zhang, S. Zhang, G. Pan, Using a fractional-order PID controller to provide robust yaw control for autonomous undersea vehicles, Ocean Eng., 257 (2022). One
[35] Fractional difference calculus, K. S. Miller, B. Ross, In: Univalent functions, fractional calculus, and its applications, Horwood, Chichester, 1989, 139–152. The new integral transform "Mohand Transform" was introduced by M. Mohand and A. Mahgoub in Adv. Theor. Appl. Math., 12 (2017), 113–120. 2.1 [37] S. Momani and Z. Odibat, Analytical solution of a time-fractional Navier-Stokes equation using Adomian decomposition approach, Appl. Math. Comput., 177 (2006), 488–494. Int. J. Numer. Methods Heat Fluid Flow, 31 (2021), 3490–3504 2.2 M. Nadeem, J.-H. He, and A. Islam, The homotopy perturbation approach for fractional differential equations: Part 1 Mohand transform.
[39]J. Spanier, K. Oldham, The theory and applications of differentiation and integration to arbitrary order in the fractional calculus, Academic Press, New York, 1974. One
[40]Fractional differential equations by I. Podlubny, Academic Press, San Diego, CA, 1999. One
[41]P. Veeresha, D. G. Prakasha, H. M. Baskonus, Hepatitis E virus dynamics analysis utilizing the Atangana-Baleanu fractional derivative, Eur. Phys. J. Plus, 134 (2019), 1–11. 1 [42]M. Goyal, D. G. Prakasha, P. Veeresha, A. Prakash, The q-homotopy analysis transform method is a novel effective approach for solving fractional coupled Navier-Stokes equations, Pramana – J. Phys., 93 (2019), 1–10. 1 [43]A. A. Ragab, K. M. Hemida, M. S. Mohamed, M. A. Abd El Salam, Using the homotopy analysis approach to solve the time-fractional Navier-Stokes equation, Gen. Math. Notes, 13 (2012), 13–21. 1 [44]B. Ross, Fractional Calculus and Its Applications, Springer, Berlin, (2006), 1–36. A short history and explanation of the basic theory of fractional calculus. 1 [45] The Mohand transforms and their applications for solving differential equation systems, written by R. Saadeh, A. A. Alshawabkeh, R. Khalil, M. A. Abdoon, N. E. Taha, and D. K. Almutairi, Eur. J. Pure Appl. Math., 17 (2024), 385–409. 1 [46] O. I. Marichev, A. A. Kilbas, S. G. Samko, Gordon and Breach Science Publishers, Yverdon, Fractional Integrals and Derivatives (1993). A. Khan, R. Shah, J. Kafle, I. Mahariq, F. Jarad, P. Sunthrayuth, R. Ullah, A. Khan, R. J. Funct. Spaces, 2021 (2021), 10 pages; Numerical study of the fractional-order nonlinear system of Volterra integro-differential equations. 1 [48] New research for general fractional financial models of awareness and trial advertising choices, by N. H. Sweilam, M. M. Abou Hasan, and D. Baleanu, Chaos Solitons Fractals, 104 (2017), 772–784. 1 [49] P. Veeresha, D. G. Prakasha, Two dependable methods for solving fractional Zakharov-Kuznetsov equations, Chinese J. Phys., 60 (2019), 313–330. 1 [50] MAP-based modeling approach and performance analysis of a task offloading scheme with time-correlated traffic and virtual machine repair in MEC systems, Wireless Network, 29 (2023), 47–68. 1 [51] Y. Wang, X. Han, S. JinVariational iteration technique for fractional calculus—a general approach using Laplace transform, G.-C. Wu, D. Baleanu, Adv. Differ. Equ., 2013 (2013), 9 pages. One

[52]IEEE Antennas Wirel. Propag. Lett., 21 (2021), 656–660; Y. Xi, W. Jiang, K. Wei, T. Hong, T. Cheng, and S. Gong, Wideband RCS reduction of microstrip antenna array employing coding metasurface with low Q resonators and quick optimization technique